Water Practice & Technology

IWA PUBLISHING

Water Practice & Technology Vol 17 No 9, 1881 doi: 10.2166/wpt.2022.096

Determination of mefenamic acid in aqueous solutions using merging zone – continuous flow injection

Lubna Al-Ameer[a,*], Kadhim K. Hashim[b] and Dakhil Nassir Taha[a]

[a] Chemistry Department of the College of Science for Women, Babylon University, Babylon, Iraq
[b] College of Environment Science, AlQasim Green University, Babylon, Iraq
*Corresponding author. E-mail: wsci.lubna.alameer@uobabylon.edu.iq

ABSTRACT

This research aims at using a novel algorithm to determine the concentration of mefenamic acid (MA) in solutions using merging zone-continuous flow injection. The MA concentration in aqueous solutions was determined using this technology, and the results obtained using this method were compared to those obtained using more conventional methods. All flow injection analyses were carried out utilizing a Rheodyne valve 7725, a Rabbit peristaltic pump, a BioLogic QuadTec UV-Vis Detector, and a Sartorius CPA2P Competence Analytical Balance, as well as a Sartorius CPA2P Competence Analytical Balance. The data is then received by a signal detector and a specialized software spectrometer. A spectroscopic scan is used to determine the maximum wavelength of the product, a calibration curve is created, and measurements are taken to estimate the drug's absolute concentrations in aqueous solutions. The detection and quantitative limits were set to 0.021 and 0.071 parts per million. This treatment is popular and could be a good alternative to conventional methods because it is simple, rapid, precise, inexpensive, and adaptable.

Key words: flow injection analyses, mefenamic acid, version 15 of the G-chrom software, zone of consolidation

HIGHLIGHTS

- A novel merging zone-continuous flow injection was used to measure the mefenamic acid in solutions.
- The obtained detection and quantitative limits were set to 0.021 and 0.071 parts per million.
- This method could be a good alternative to the conventional methods because it is simple, rapid, precise, inexpensive, and adaptable.

1. INTRODUCTION

In past decades, aquatic pollution by residual pharmaceuticals and personal care products (PPCPs) have been a major concern. Discharges from wastewater treatment plants (WWTPs) have been recognized as one of the most important sources of PPCPs. Previous reports have detected PPCPs in aquatic environments such as wastewater effluent, rivers, and fish samples. Although concentrations of many PPCPs in natural aquatic environments are generally in the range from parts per trillion (ng L1) to parts per billion (μg L1), several compounds have been shown to remain in environments at levels that can pose potential ecological risks (Sankoda *et al.* 2019). Among PPCPs, mefenamic acid (MA) is a nonsteroidal anti-inflammatory drug (NSAID) that belongs to the medications' anthranilic acid derivatives (or fenamate) class and has been frequently detected in aquatic environments due to the low removal efficiency of WWTP processes. It treats mild to moderate pain and is a member of the anthranilic acid derivatives (or fenamate) family (Morcoss *et al.* 2017). It is not extensively used in the United States because of its adverse side effects and expensive cost compared to other NSAIDs (García *et al.* 2001; Savjani *et al.* 2017). Specifically, it is known by the scientific name dimethylphenylaminobenzoic acid, which is the name derived. It was first made available to the public by Parke-Davis in the 1960s, and it has since been widely distributed. Meftal is a brand name for a medication genericized in the 1980s and available under various brand names. Those who have previously experienced allergic reactions such as urticaria and asthma in response to this or other NSAIDs (for example, aspirin), those who have peptic ulcers or chronic inflammation of the digestive tract, those who have kidney or liver disease, and those who are pregnant or breastfeeding should not take this medication (Cimolai 2013). MA has been linked to minor side effects (Ozgoli *et al.* 2009), including

headaches, anxiety, nausea, and vomiting. Although toxic epidermal necrolysis and blood cell abnormalities such as agranulocytosis are rare side effects, they can be life-threatening. Because of this, acute liver injury has been linked to the condition over time (Sabry 1998). The term 'premature closure of the ductus arteriosus during pregnancy' was added to the label in the United States in 2008 (Gewillig *et al.* 2009). Because of low amniotic fluid levels in pregnant women (Ovayolu *et al.* 2020), by October 2020, the FDA has mandated that all NSAIDs be amended to contain a warning about the risk of renal problems in unborn neonates (Gewillig *et al.* 2009). Women who are 20 weeks or more pregnant, according to experts, should avoid taking NSAIDs (Gewillig *et al.* 2009). This medication's interactions with other NSAIDs are comparable to those of those other medications (NSAIDs). MA has been shown to interfere with the anti-clotting activity of aspirin. Its ability to separate warfarin and phenprocoumon from plasma proteins enhances its anticoagulant properties. Some studies have linked inflammatory drugs such as corticosteroids and selective serotonin reuptake inhibitors to an increased risk of gastrointestinal ulcers. If the amount of methotrexate and lithium excreted by the kidneys is reduced, this may have negative repercussions. The toxicity of cyclosporin and tacrolimus may be exacerbated by using this medicine. Inhibitors, sartans, and diuretics are antihypertensive drugs that have reduced efficacy when combined with these other medications, and the risk of kidney damage is increased (de Abajo *et al.* 1999; de Abajo 2011).

The treatment approaches of MA from wastewater are not limited to electro-Fenton degradation (Dolatabadi *et al.* 2020), activated charcoal, and a micelle-clay complex (Khalaf *et al.* 2013), chlorine dioxide (Hey *et al.* 2012), biological treatment (Hata *et al.* 2010; Rosal *et al.* 2010; Deepa *et al.* 2021), membranes (Kimura *et al.* 2005; Radjenović *et al.* 2009) and oxidation (Colombo *et al.* 2016; Deepa *et al.* 2021). Additionally, the electrochemical method is attracting the attention of researchers because of its cheapness (Hashim *et al.* 2021b; Arab *et al.* 2022) and environmental safety (Abdulhadi *et al.* 2021; Hashim *et al.* 2021a); therefore, it can be a suggestion in this paper for removing MA from wastewater.

Many approaches for assessing MA in pharmaceutical formulations and biological materials have been developed and published. A few examples of these approaches are chemiluminescence, catalytic degradation (Amini & Mengelizadeh 2020), electrochemical sensors (Hasanzadeh *et al.* 2012; Bukkitgar *et al.* 2014; Valian *et al.* 2022), spectrophotometry, spectrofluorometry, high-performance liquid chromatography (HPLC) and capillary electrophoresis (CE) (Ahrer *et al.* 2001; Jaiswal *et al.* 2007; Madrakian *et al.* 2009). As a result, the current research is focused on detecting the concentration of MA in aqueous solutions utilizing a flow injection approach and new software created by (Al Sultani *et al.* 2019), branded G-chrom V1.5, which was just released.

2. MATERIALS AND METHODS

2.1. Reagents and substances

Unless otherwise stated, all analytical-grade chemicals were used, and double-distilled water was used for all processes from reagent dilution to sample processing. The reference 1,2-naphthoquinone-4-sulfonate (NQS) provided by Aldrich, and the drug was obtained from Samara, an Iraqi state-owned pharmaceutical enterprise (SDI).

2.2. Preparation of MA, NQS, and experimental work

It was possible to make MA at a concentration of 50 parts per million (ppm) by dissolving 5 mg (0.005 gm) of MA in 25 mL distilled water and diluting the solution with distilled water 100 mL in a volumetric flask. All of the dilutions shown below were created using freshly produced working solutions. By dissolving it in 50 mL of distilled water, sodium NQS 5 mg (0.005 gm) of the reagent was freshly prepared as a stock solution containing 100 ppm. 0.2 M sodium hydroxide is used in this recipe. To make it, dissolve 1.6 gm sodium hydroxide in 25 mL distilled water in a volumetric flask and dilute to 200 mL with more distilled water. 0.2 M potassium chloride is used in this experiment. To make a standard solution, dissolve 2.858 gm in 20 mL distilled water in a volumetric flask and dilute it with distilled water to 200 mL in a volumetric flask. 0.2 M boric acid is used in this recipe. Therefore, it was necessary to prepare a standard solution of 1.2366 gm by dissolving it in 25 mL of distilled water and diluting it to 100 mL in a volumetric flask before using it.

Solution of sodium hydroxide and boric acid as a buffer 50 mL distilled water was used to dissolve the boric acid, which was then combined with 4.15 mL sodium hydroxide (0.2 M) in a 100 mL volumetric flask to form a solution. After that, the solution was diluted with distilled water until it reached the desired concentration.

A pH 10 buffer solution containing boric acid, potassium chloride, and sodium hydrochloride was prepared in a 100 mL volumetric flask using 25 mL of boric acid (0.2 M), 25 mL of potassium chloride (0.2 M), and 21.85 mL of sodium hydroxide (0.2 M), which was then diluted with distilled water to the desired concentration.

Sodium hydroxide and potassium chloride buffer solution with a pH of 12 was prepared by combining 50 mL of potassium chloride (0.2 M) and 24 mL of sodium hydroxide (0.2 M) in a 100 mL volumetric flask and diluted with distilled water to the desired concentration.

2.3. Instruments

All flow injection analyses were carried out utilizing a Rheodyne valve 7725, a Rabbit peristaltic pump, a Bio-Logic QuadTec UV-Vis Detector, and a Sartorius CPA2P Competence Analytical Balance, as well as a Sartorius CPA2P Competence Analytical Balance. G-Chrom V1.5 loop volume is 40 litres for appropriate analytical methods that can be designed and developed for a variety of purposes, such as qualitative analysis, formulation, conservatism content, and estimating analyte concentrations in biological or non-biological fluids. The software designer is responsible for the methods' scanning, calibration, measurements, and report editing.

It was decided to use accumulated peak analysis (APA) because of its precision, quick analysis, and ability to graph data. The data produced from the technique were screened and compared to the standard solution with the help of an equation that was expressly created for this purpose. This step will aid the analyst in understanding the parameters that influence the performance of the analysis during the next stage. As shown in Figure 1, the FIA injection system comprises a peristaltic pump and an injection valve joined together by a single low-load link to deliver the fluid. Operation is comparable to a standard six-way valve operating in two directions, which is widely applied in the spectrum analysis of injection techniques, except that this injection system operates in one direction only. The injection ring comprises a single input and output connected by many channels. A two-link valve regulates the condition of the injection system and helps to enhance modelling by controlling the flow of fluid. The diameter of the injection ring (the loading link) used in this experiment, which is μ50 L, determines the size of the sample taken.

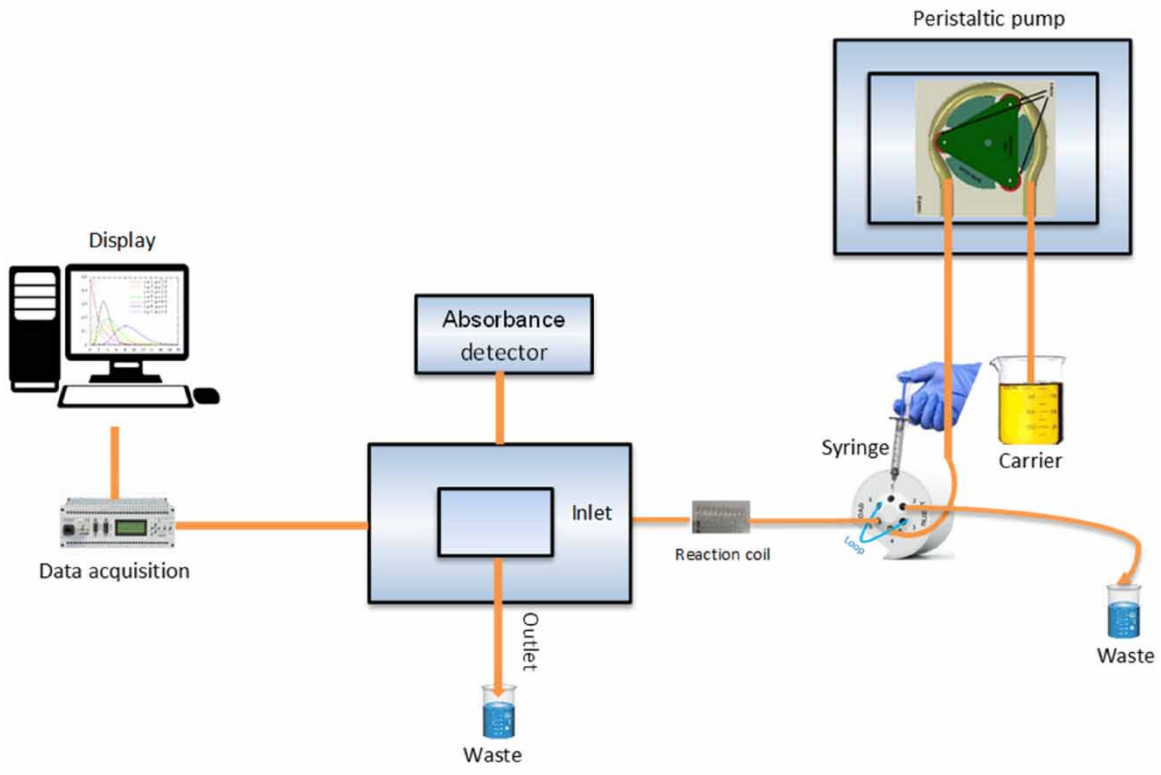

Figure 1 | A flow injection system model that our laboratory designed and built.

3. RESULTS

3.1. Determine the maximum wavelength (max)

1 mL of a standard solution containing 50 ppm MA was transferred to a 10 mL volumetric flask, followed by 1 mL of buffer solution (pH 12) and 1 mL of NQS solution. Finally, 1 mL of a standard solution containing 50 ppm MA was added (100 ppm). The components were combined and diluted with distilled water to ensure proper mixing.

A study was conducted to investigate the absorption spectra of MA and compare it to water; it was discovered that MA exhibits a maximum absorption peak at 285 nm. It was determined that there was no absorption interference between the reagent and the sample by examining the absorption spectrum of NQS against water in the range of wavelengths used in the experiment (385 580). Then, the absorption spectra of the product were compared to those of water (to confirm that there was no effect of the reagent in this range). Finally, the absorption spectra of the result were compared to those of the reagent to determine their differences. The maximum absorption wavelength of the product was determined to be 477 nm in length (Figure 2 and Table 1).

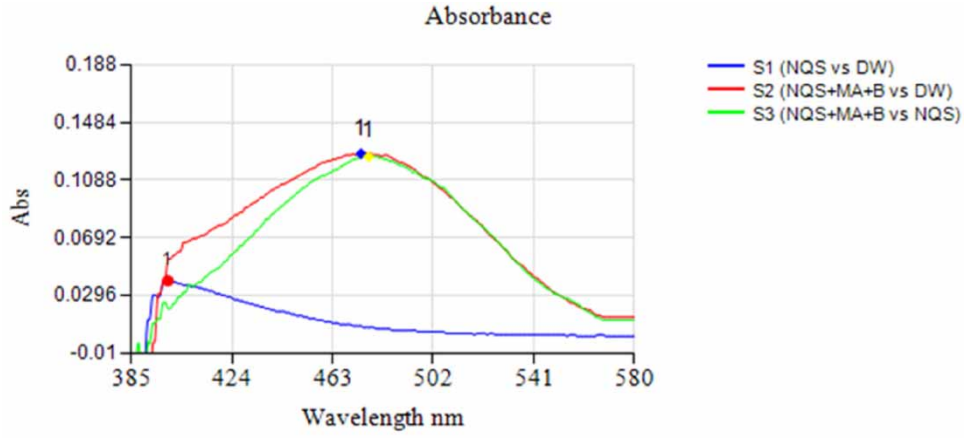

Figure 2 | The spectrum of NQS and product.

Table 1 | Result of lambda max

Lambda	S1	Lambda	S2	Lambda	S3
399	0.04	474	0.127	477	0.125

3.2. Optimization of experimental conditions

To select the best potential experimental conditions for the experiment, a single parameter was adjusted, and the impact on the absorbance of the coloured species was measured.

3.2.1. The influence of flow rate

The effect of flow rate on the formation of the coloured product was explored by altering the flow rate and measuring the absorbance of the coloured product produced. The study discovered that the optimal flow rate is 3 = 1.5 ml/min, generating the best beak shape and the most significant absorption. Two were chosen above the other possibility due to the superior time required by speed, as shown in Figure 3.

3.2.2. The following is the effect of the length of the mixing coil

The effect of altering the length of the reaction coil was explored, and the results were compared to those obtained without a mixing coil in the experiment. Several lengths (100, 75, 50, and 25 cm) were used to test

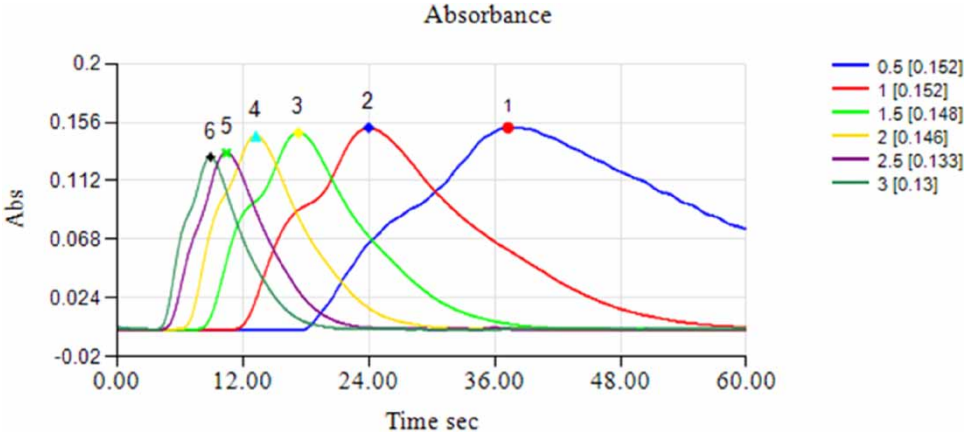

Figure 3 | Effect of flow rate.

the response without using a response coil. The peak with the highest absorbency value and the best shape was obtained using a reaction coil with a length of 25 cm after the double-top peak, which indicates that the mixing was not complete, was eliminated as a low peak indicating insufficient mixing and a high peak indicating adequate mixing being obtained (see Figure 4).

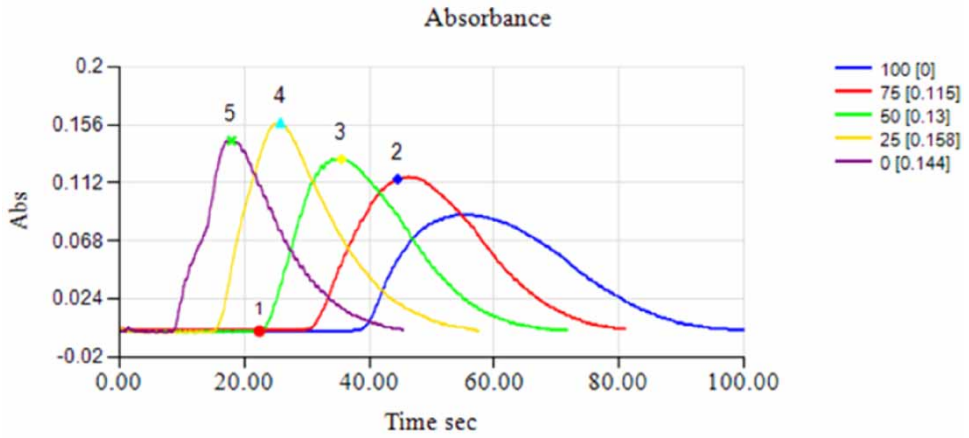

Figure 4 | The impact of the reaction coil is depicted.

3.2.3. The following is the effect of the base type and the quantity added

Several base solutions, such as sodium hydroxide and multiple buffer solutions with varied pH values (9, 10, and 12), were utilized to establish the maximal absorbance intensity. In this study, NaOH is utilized since it has a higher sensitivity and repeatability than methanol (see Figure 5). However, the optimal sodium hydroxide concentration for creating the most remarkable colour intensity was identified to be 0.5 mL for each 100 ml sample, which was shown to be the case (see Figure 6).

3.2.4. Effect of NQS concentration

This study evaluated the effect of changing the reagent concentration on the reaction. A range of NQS concentrations (10 ppm to 100 ppm) was used to collect data, and the results revealed that the best absorbance occurs when the reagent concentration is 50 ppm (see Figure 7).

To create solutions of varying MA concentrations for injection with 50 ppm NQS as carrier solution, 25 cm of reaction coil, and a flow rate of 1.5 mL/min, 20-mL volumetric flasks with a capacity of 0.1 mL sodium hydroxide solution were utilized. The flow rate was 1.5 mL/min. The calibration curve shown below was created using the steps presented in Figures 8 and 9.

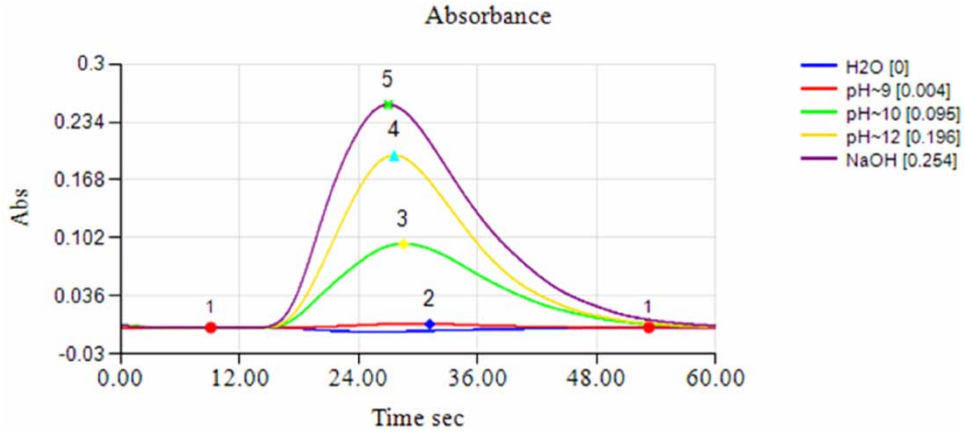

Figure 5 | The Influence of the base type.

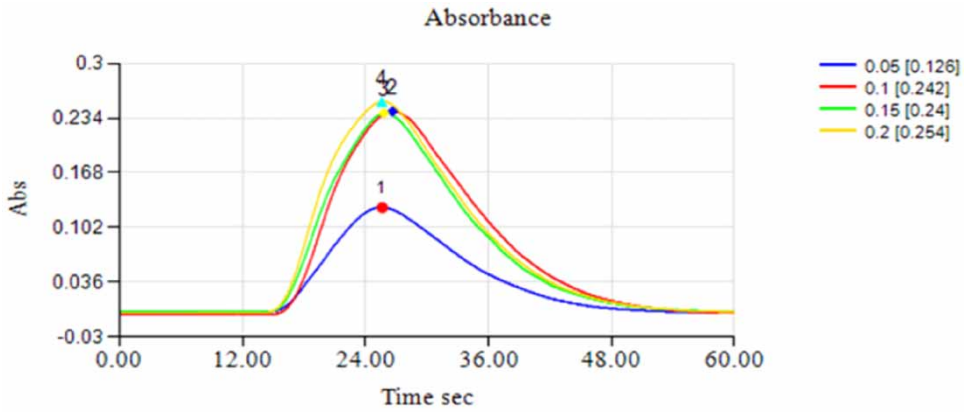

Figure 6 | Effect of base concentration on the results.

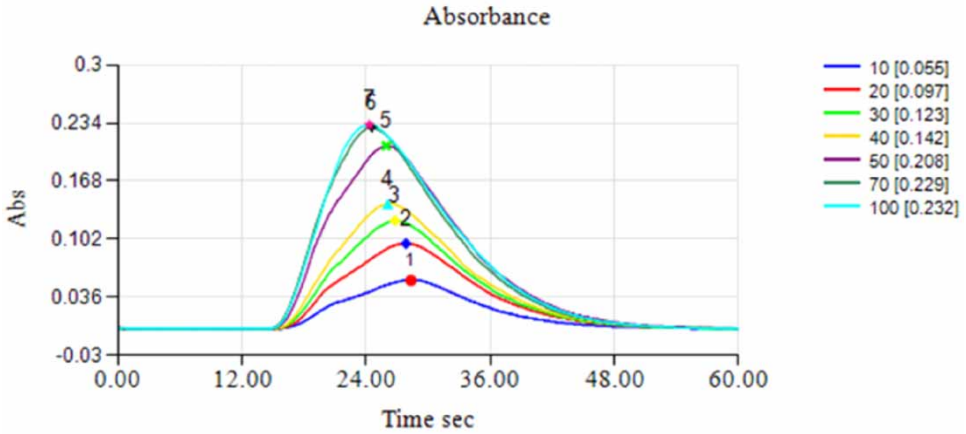

Figure 7 | Influence of NQS concentration.

3.3. Repeatability

By doing multiple tests on six sample solutions containing 13 ppm MA, it was revealed that the repeatability of the suggested approach was extremely excellent. The method demonstrated a high degree of reproducibility (see Figure 10 and Table 2).

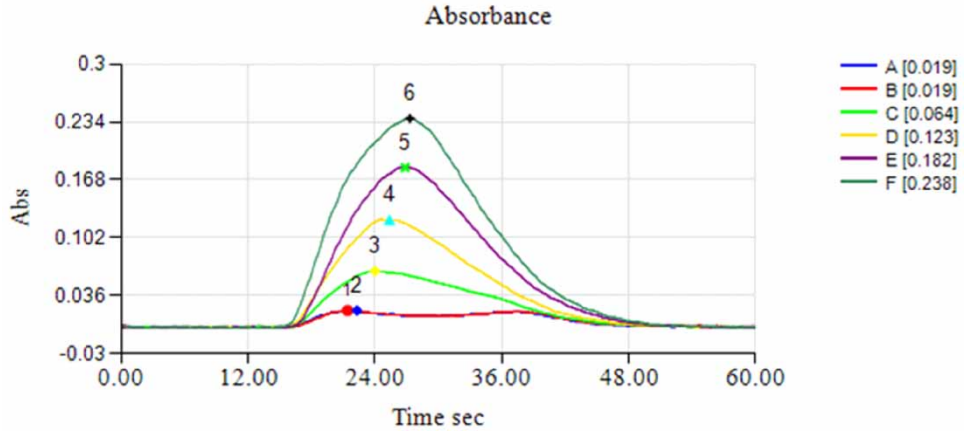

Figure 8 | The 1–20 ppm spectrum of MA.

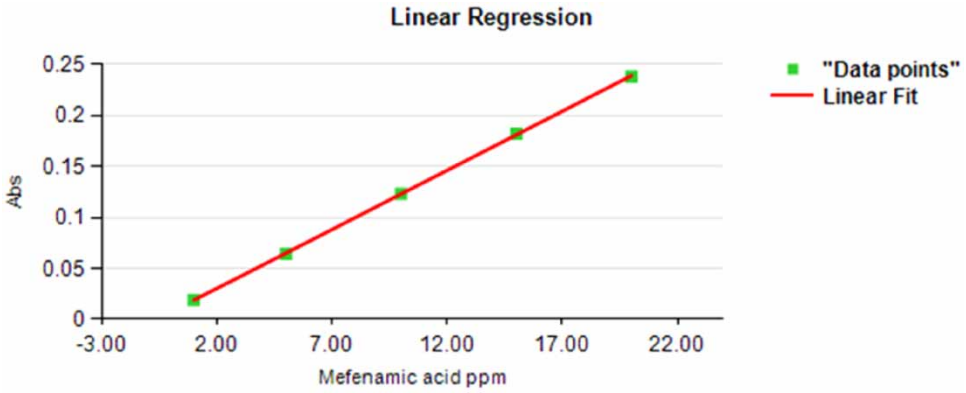

Figure 9 | Calibration curve of MA.

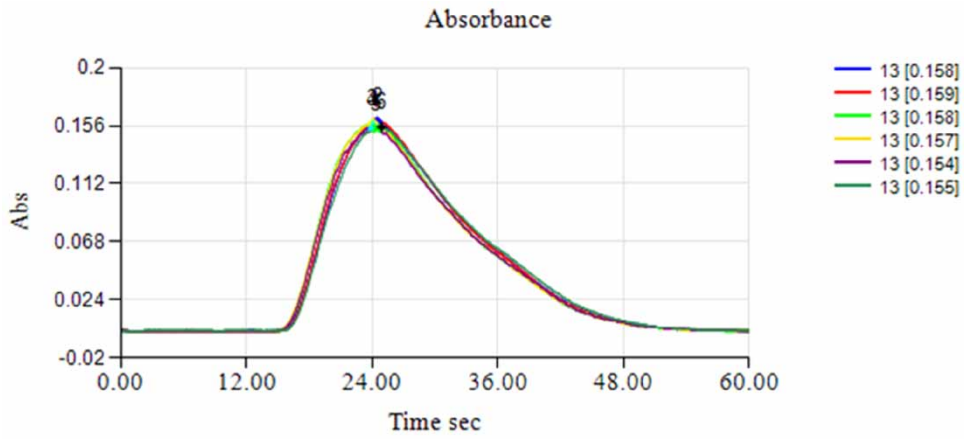

Figure 10 | The reproducibility of MA.

3.4. Dead volume

The dead volume was computed to verify the system's high quality as a consequence of the three findings demonstrating that no interaction happened when the base, sample, and reagent were eliminated (see Figure 11).

Table 2 | Result of absorbance

Index	Sample	MA ppm	Peak Height
1	A	1	0.019
2	B	1	0.019
3	C	5	0.064
4	D	10	0.123
5	E	15	0.182
6	F	20	0.238

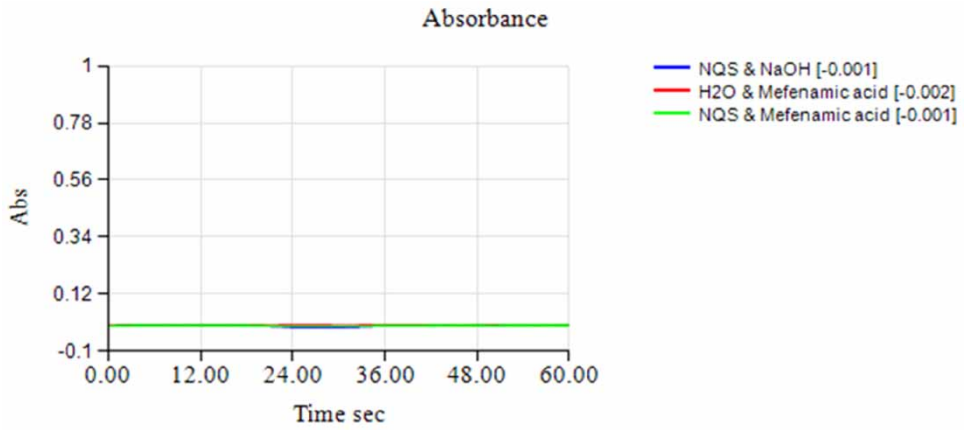

Figure 11 | The dead volume of MA.

3.5. The determination of dispersion

The MA is present at 20 ppm. Two experiments were carried out to estimate the dispersion value within the sample zone. For the first experiment, a concentration of MA (20 ppm) is injected into the FIA. The result of this experiment represents the intensity response of the sample injected into the experiment (H max). After the reactants (MA and NQS) have been combined and transmitted through a manifold unit, the reaction is constant, exhibiting no dispersion effect due to convection or diffusion. This illustration depicts the Ho. It is possible to compute dispersion (D) by applying the following equation: D ° = Ho/H max ((D = 1.15). The dispersion of these figures is restricted to a small range (see Figure 12 and Table 3).

3.6. In aqueous solutions, MA can be determined as follows

Three aqueous solutions were prepared and used as solutions of unknown concentrations; then, the absorbance was measured according to the optimum conditions, as shown in Figure 13.

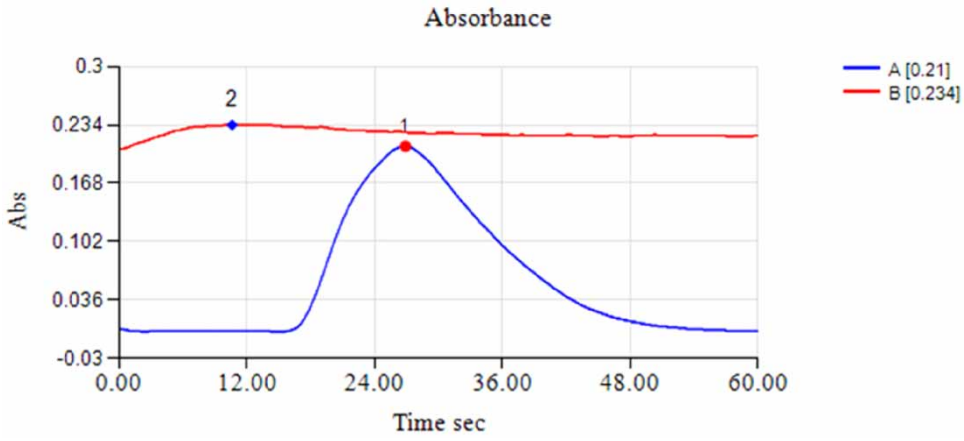

Figure 12 | Dispersion.

Table 3 | Equation and R-squared value with ideal values of a calibration curve

MA ppm	Abs	QR
1	0.019	0.019
1	0.019	0.019
5	0.064	0.065
10	0.123	0.123
15	0.182	0.181
20	0.238	0.239

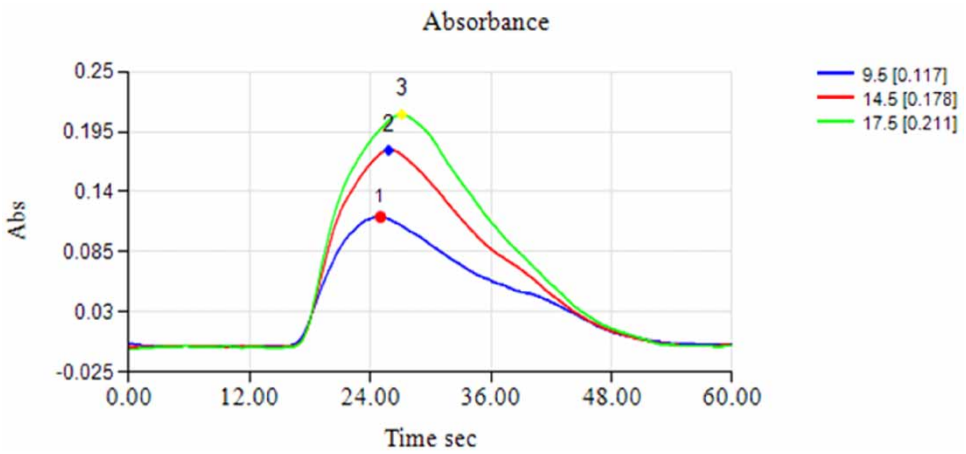

Figure 13 | The spectrum of possible applications.

Then the solutions' concentration was determined by setting each solution's absorbance on the straight line of the previous calibration curve, as shown in Table 4 and Figure 14. The value of the calculated results from the calibration curve was very close to those of the prepared solutions.

Table 4 | Value of sample application

Index	Taken	Founded	Peak Height
1	9.5	9.457	0.117
2	14.5	14.767	0.178
3	17.5	17.554	0.211

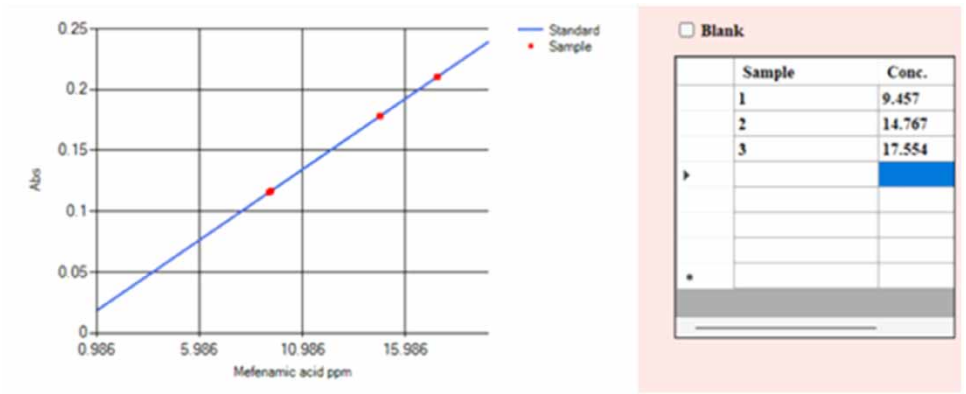

Figure 14 | Determination of sample unknown on a calibration curve.

4. DISCUSSION

The technique is based on the physical characteristics of electromagnetic radiation. The study indicated that the simple injection technique could detect drug concentrations in aqueous solutions. According to the findings, the detection limit was determined to be LOD = 0.021 ppm, the limit of quantification was determined to be LOQ = 0.071 ppm, the straight-line equation for drug concentration versus absorption was determined to be $y = 0.012\ x + 0.007$, and the correlation equation for the standard specification 0.9999 linearities was determined to be in the range of 2–20 ppm. The calibration curve findings showed a high correlation coefficient with linearity, showing a strong association between peak height and concentration, which is important to the study's objectives. G-Chrome is APA for this type of analysis. The analysis was conducted based on a single reading. This method is both quick and precise.

Along with the standard deviation (SD) and relative standard deviation (RSD%), this method gave the analyst greater latitude in computing the SD. The data, graphs, and tables were merged into a final, extremely trustworthy report by computing the equations of straight and linear lines without using normal Excel computations. Compared to non-destructive methods and near-infrared spectroscopy, the results from this method are acceptable (NIRS).

MA has no long-term or fatal effects, but it might cause health problems if ingested in excess. MA has been shown to interfere with the anticoagulant activity of aspirin. Some studies have linked anti-inflammatory medications to an increased incidence of stomach ulcers. When used with diuretics, the efficacy of the diuretics is decreased, and the risk of kidney damage increases. The FDA in the United States has ordered a review of all NSAIDs to warn about the potential for kidney issues in newborns. Several techniques are employed in drug detection and identification, including differential pulse polarization, thin layer chromatography, adsorption voltammetry, and differential spectroscopy. The laboratory tests and G-Chrome program are more precise, adaptable, and time-efficient when constructed on measurements. This technique cumulatively records the individual measurements of each sample throughout time. This approach necessitates less analysis time than collecting all of the statistical data necessary to produce the final report. This pattern might be appropriate for indicators. Routine measurements are utilized in spectroscopic analysis to determine flow and injection. In conclusion, the newly developed G-Chrome method is inapplicable to solid samples. On the other hand, solid samples can be dissolved in a solvent tested against G-Chrome.

For future developments, new sensors could be integrated into this technique, such as electromagnetic sensors nanosensors (Shojaei *et al.* 2016; Ryecroft *et al.* 2019, 2021; Mohammadian *et al.* 2022) or membrane sensors (Babakhanian 2012; Noroozi & Keypour 2017).

5. CONCLUSIONS

A paradigm shift has occurred in the visual evolution of FI-UV. Unlike previous instruments, the new one employs a novel, constructed, in-laboratory planned, and in-laboratory managed G-Chrome flow-injection software to determine the spectroscopic approach. This technology is simple to operate, and data transfer is automated. Because of the internal design of the software used in this approach, injecting a sample and then repeating it at an intersection or altering the sample are simple. Additionally, it was discovered that the data acquired was accurate and equivalent to that produced using more complex instruments. This system distinguishes itself via its low cost and ease of use, high degree of flexibility, precision, and control over the findings, and, most importantly, the analyst's capacity to construct and improve the system and methodology.

For future developments, new sensors could be integrated into this technique, such as electromagnetic or membrane sensors.

DATA AVAILABILITY STATEMENT

Data cannot be made publicly available; readers should contact the corresponding author for details.

CONFLICT OF INTEREST

The authors declare there is no conflict.

REFERENCES

Abdulhadi, B., Kot, P., Khalid, H., Shaw, A., Muradov, M. & Al-Khaddar, R. 2021 Continuous-flow electrocoagulation (EC) process for iron removal from water: experimental, statistical and economic study. *Science of the Total Environment* **760**(2), 1–16.

Ahrer, W., Scherwenk, E. & Buchberger, W. 2001 Determination of drug residues in water by the combination of liquid chromatography or capillary electrophoresis with electrospray mass spectrometry. *Journal of Chromatography A* **910**(1), 69–78.

Al Sultani, K. K. H. A.-R., Mohmmed Al-Samrrai, A. A. & Shatha, Y. 2019 Determination of tartrazine and sodium benzoate as food additives in some local juices using continuous flow injection analysis. *Engineering in Agriculture, Environment and Food* **12**(2), 217–221.

Amini, M. M. & Mengelizadeh, N. 2020 Catalytic degradation of mefenamic acid by peroxymonosulfate activated with MWCNTs-CoFe2O4: influencing factors, degradation pathway, and comparison of activation processes. *Environmental Science and Pollution Research* **27**(36), 45324–45335.

Arab, M., Faramarz, M. G. & Hashim, K. 2022 Applications of computational and statistical models for optimizing the electrochemical removal of cephalexin antibiotic from water. *Water* **14**(3), 344–359.

Babakhanian, A. 2012 A novel Pt (bipy) 2Cl2-Poly (vinyl chloride) membrane sensor for mefenamic acid detection in pharmaceutical and. *Sensor Letters* **10**, 1–6.

Bukkitgar, S. D., Shetti, N. P., Nayak, D. S., Bagehalli, G. B. & Nandibewoor, S. T. 2014 Electrochemical sensor for the detection of mefenamic acid in pharmaceutical sample and human urine at glassy carbon electrode. *Der Pharma Chemica* **6**(2), 258–268.

Cimolai, N. 2013 The potential and promise of mefenamic acid. *Expert Review of Clinical Pharmacology* **6**(3), 289–305.

Colombo, R., Ferreira, T. C. R., Ferreira, R. A. & Lanza, M. R. V. 2016 Removal of mefenamic acid from aqueous solutions by oxidative process: optimization through experimental design and HPLC/UV analysis. *Journal of Environmental Management* **167**, 206–213.

de Abajo, F. J. 2011 Effects of selective serotonin reuptake inhibitors on platelet function. *Drugs & Aging* **28**(5), 345–367.

de Abajo, F. J. R., Montero, L. A. G. & Montero, D. 1999 Association between selective serotonin reuptake inhibitors and upper gastrointestinal bleeding: population based case-control study. *Bmj* **319**(7217), 1106–1109.

Deepa, R., Madhu, G. & Thomas, R. M. 2021 A comparative study on the removal of an emerging contaminant mefenamic acid from aqueous media by various advanced oxidation methods. *Materials Today: Proceedings* **47**, 1416–1422.

Dolatabadi, M., Ahmadzadeh, S. & Ghaneian, M. T. 2020 Mineralization of mefenamic acid from hospital wastewater using electro-Fenton degradation: optimization and identification of removal mechanism issues. *Environmental Progress & Sustainable Energy* **39**(3), e13380.

García, S., Sánchez-Pedreño, C., Isabel, A. & Concepción, G. 2001 Flow-injection spectrophotometric determination of diclofenac or mefenamic acid in pharmaceuticals. *Microchimica Acta* **136**(1), 67–71.

Gewillig, M., Brown, S. C., De Catte, L., Debeer, A., Eyskens, B., Cossey, V., Van Schoubroeck, D., Van Hole, C. & Devlieger, R. 2009 Premature foetal closure of the arterial duct: clinical presentations and outcome. *European Heart Journal* **30**(12), 1530–1536.

Hasanzadeh, M., Shadjou, N., Saghatforoush, L. & Dolatabadi, J. E. N. 2012 Preparation of a new electrochemical sensor based on iron (III) complexes modified carbon paste electrode for simultaneous determination of mefenamic acid and indomethacin. *Colloids and Surfaces B: Biointerfaces* **92**, 91–97.

Hashim, K., Al-Rifaie, J. K., Aljaaf, A. J., Idowu, I., Amoako-Attah, J. & Nikitas, G. 2021a RSM (Response Surface Methodology) modelling of inter-electrodes spacing effects on phosphate removal. In: *2021 14th International Conference on Developments in eSystems Engineering (DeSE)* (Al-Jumeily, D. ed.). IEEE, Sharjah, United Arab Emirates, pp. 586–589.

Hashim, K. S., Shaw, A., AlKhaddar, R., Kot, P. & Al-Shamma'a, A. 2021b Water purification from metal ions in the presence of organic matter using electromagnetic radiation-assisted treatment. *Journal of Cleaner Production* **280**(2), 1–17.

Hata, T., Kawai, S., Okamura, H. & Nishida, T. 2010 Removal of diclofenac and mefenamic acid by the white rot fungus Phanerochaete sordida YK-624 and identification of their metabolites after fungal transformation. *Biodegradation* **21**(5), 681–689.

Hey, G., Ledin, A., Jansen, J. l. C. & Andersen, H. R. 2012 Removal of pharmaceuticals in biologically treated wastewater by chlorine dioxide or peracetic acid. *Environmental Technology* **33**(9), 1041–1047.

Jaiswal, Y. T., Talele, G. & Surana, S. 2007 Application of HPLC for the simultaneous determination of ethamsylate and mefenamic acid in bulk drugs and tablets. *Journal of Liquid Chromatography & Related Technologies* **30**(8), 1115–1124.

Khalaf, S., Al-Rimawi, F., Khamis, M., Nir, S., Bufo, S. A., Scrano, L., Mecca, G. & Karaman, R. 2013 Efficiency of membrane technology, activated charcoal, and a micelle-clay complex for removal of the acidic pharmaceutical mefenamic acid. *Journal of Environmental Science and Health, Part A* **48**(13), 1655–1662.

Kimura, K., Hara, H. & Watanabe, Y. 2005 Removal of pharmaceutical compounds by submerged membrane bioreactors (MBRs). *Desalination* **178**(1), 135–140.

Madrakian, T. A., Afkhami, A. & Mohammadnejad, M. 2009 Second-order advantage applied to simultaneous spectrofluorimetric determination of paracetamol and mefenamic acid in urine samples. *Analytica Chimica Acta* **645**(1–2), 25–29.

Mohammadian, E., Rahimpour, E., Alizadeh-Sani, M., Foroumadi, A. & Jouyban, A. 2022 An overview on terbium sensitized based-optical sensors/nanosensors for determination of pharmaceuticals. *Applied Spectroscopy Reviews* **57**(1), 39–76.

Morcoss, M. M. A., Ali, N. S., Elsaady, N. W. & Mohammed, T. 2017 Different chromatographic methods for simultaneous determination of mefenamic acid and two of its toxic impurities. *Journal of Chromatographic Science* **55**(7), 766–772.

Noroozi, M. & Keypour, H. 2017 Novel mefenamic acid PVC membrane sensor based on a new Cd Schiff's base complex containing a phenanthroline unit. *RSC Advances* **7**(62), 39118–39126.

Ovayolu, A. O., Karaman, G., Yuce, E., Ozek, T., Turksoy, M. A. & Vugar, A. 2020 Amniotic fluid levels of selected trace elements and heavy metals in pregnancies complicated with neural tube defects. *Congenital Anomalies* **60**(5), 136–141.

Ozgoli, G. G. & Marjan Moattar, F. 2009 Comparison of effects of ginger, mefenamic acid, and ibuprofen on pain in women with primary dysmenorrhea. *The Journal of Alternative and Complementary Medicine* **15**(2), 129–132.

Radjenović, J., Petrović, M. & Barceló, D. 2009 Fate and distribution of pharmaceuticals in wastewater and sewage sludge of the conventional activated sludge (CAS) and advanced membrane bioreactor (MBR) treatment. *Water Research* **43**(3), 831–841.

Rosal, R., Rodríguez, A., Perdigón-Melón, J. A., Petre, A., García-Calvo, E., Gómez, M. J., Agüera, A. & Fernández-Alba, A. R. 2010 Occurrence of emerging pollutants in urban wastewater and their removal through biological treatment followed by ozonation. *Water Research* **44**(2), 578–588.

Ryecroft, S. P., Shaw, A., Fergus, P., Kot, P., Hashim, K. & Conway, L. 2019 A novel gesomin detection method based on microwave spectroscopy. In *12th International Conference on Developments in ESystems Engineering (DeSE)*, Kazan, Russia, pp. 429–433.

Ryecroft, S., Shaw, A., Fergus, P., Kot, P., Hashim, K., Tang, A., Moody, A. & Conway, L. 2021 An implementation of a multi-hop underwater wireless sensor network using bowtie antenna. *Karbala International Journal of Modern Science* **7**(2), 113–129.

Sabry, S. M. 1998 Determination of flufenamic and mefenamic acids in pharmaceutical preparations using organized media. *Analytica Chimica Acta* **367**(1), 41–53.

Sankoda, K. S., Sugawara, Y., Aida, T., Yamamoto, C., Kobayashi, J., Sekiguchi, K. & Wang, Q. 2019 Aqueous photochemical degradation of mefenamic acid and triclosan: role of wastewater effluent matrices. *Water Science and Technology* **79**(10), 1853–1859.

Savjani, J. K., Mulamkattil, S., Variya, B. & Patel, S. 2017 Molecular docking, synthesis and biological screening of mefenamic acid derivatives as anti-inflammatory agents. *European Journal of Pharmacology* **801**, 28–34.

Shojaei, S., Nasirizadeh, N., Entezam, M., Koosha, M. & Azimzadeh, M. 2016 An electrochemical nanosensor based on molecularly imprinted polymer (MIP) for detection of gallic acid in fruit juices. *Food Analytical Methods* **9**(10), 2721–2731.

Valian, M., Khoobi, A. & Salavati-Niasari, M. 2022 Synthesis, characterization and electrochemical sensors application of Tb2Ti2O7 nanoparticle modified carbon paste electrode for the sensing of mefenamic acid drug in biological samples and pharmaceutical industry wastewater. *Talanta* **247**, 123593.

First received 4 June 2022; accepted in revised form 10 August 2022. Available online 18 August 2022